Supplemental Information

Figure 1-S1: Quantification and quality control plots of ubiquitinomics data. Related to Figure 1. Quality control plots for diGly enriched dataset were generated using the artMS Bioconductor package (version 0.9) (Jimenez-Morales *et al.*, 2019). **(A)** Percent of contaminants (CON), proteins (PROT) and reversed sequences (REV) in each experimental condition (control, dotA-1h, dotA-8h, WT-1h, WT-8h) were quantified to adjust the false-discovery-rate (FDR). **(B)** Samples were normalized across fractions by median-centering the Log2-transformed MS1 intensity distributions. **(C)** Correlation table and matrix showing the clustering of the different experimental conditions. **(D)** Principal Component analysis of normalized MS Intensities of experimental conditions (control, ΔdotA-1h, ΔdotA-8h, WT-1h, WT-8h). PC1 and PC2 captured most of the variability. Loading variables are represented as vectors. The smaller angle between control and the mutant time points (Δ*dotA*-1h, Δ*dotA*-8h) implies a larger positive correlation between them, as opposed to a lower correlation (larger angle) between the Control and the WT strain.

Figure 1-S2: Analysis of T4SS-independent (*L.p.* Δ*dotA*) changes in the host cell ubiquitinome. Related to Figure 1. (A) Counts of proteins with a significant increase (green) or decrease (magenta) in ubiquitination compared to uninfected control for Δ*dotA* 1hr and Δ*dotA* 8hr

(same data shown in Figure 1B, repeated here for clarity). **(B)** Overlap of proteins with a significant increase (green) or decrease (magenta) in ubiquitination compared to uninfected control in the 1-hour vs 8-hour *L.p*. Δ*dotA* infected conditions. **(C)** Volcano plot representation of all ubiquitinome data in Δ*dotA* vs uninfected comparison at 1- and 8-hours post-infection. Imputed values are shown as diamonds. Significance threshold is indicated by the dotted line. **(D)** Subcellular localization analysis of proteins with a significant increase or decrease in ubiquitination compared to uninfected control during *L.p*. Δ*dotA* infection for 1 or 8 hours. **(E)** Metascape pathway and protein complex analysis of proteins with a significant increase or decrease in ubiquitination compared to uninfected control during *L.p*. Δ*dotA* infection for 1 or 8 hours. Terms not significantly enriched for a given experimental condition are represented by white boxes. **(F)** Overlap of proteins with a significant increase (green) or decrease (magenta) in ubiquitination compared to uninfected control in the WT *L.p*. vs. Δ*dotA* infected conditions, at both 1- and 8-hours post-infection.

Figure 1-S3: Quantification and quality control plots of abundance data. Related to Figure 1. Identical analysis as in Figure 1S1 using abundance data.

Figure 1-S4: Analysis of *L.p.*-induced changes in host cell abundance. Related to Figure 1. Analysis of proteins with significant increases (green) or decreases (magenta) in abundance compared to uninfected control for WT and Δ*dotA* infected conditions, at both 1 and 8 hours post infection. **(A)-(D)** Comparable to analyses in Fig 1 and Fig 1S2. **(E)** Log2FC comparison of proteins with significant abundance change (grey points), significant ubiquitination change (light blue points), or both significant abundance and ubiquitination change (dark blue points) during infection with WT *L.p.* relative to uninfected control. Proteins with insignificant abundance and ubiquitination changes are shown in white. Data shown are at 1-hour post-infection (left) and 8-hours post-infection (right).

Figure 2-S1: Quantification of diGlycine site data. Related to Figure 2. Counts of diGly sites with a significant increase (green) or decrease (magenta) compared to uninfected control for the indicated infection conditions. Significance threshold: $|\log2(FC)|>1$, $p<0.05$. DiGlycine sites falling on small GTPases indicated in red.

Figure 2-S2: List of significantly regulated diGly sites falling on small GTPases. Related to Figure 2. All significantly changing diGlycine sites falling on small GTPases during WT and Δ*dotA* *L.p.* infection, organized by subfamily and infection timepoint. Cell color and number indicate Log2FC. White cells indicate no significant change. Due to the significant homology between various small GTPases, some trypsinized peptides could not be distinguished between multiple proteins. DiGlycine sites that could be assigned to multiple proteins are indicated with a "/". In our downstream analyses, we use a conservative approach and only consider the first small GTPase listed (e.g. NRAS_K147 / KRAS_K147, only NRAS_K147 is counted as a small GTPase ubiquitination site).

Figure 2-S3: Extended immunoblot analysis of small GTPase ubiquitination confirmations. Related to Figure 2. Extension of Figure 2B-E. Immunoblot analysis of lysates prepared from HEK293T FcγR cells transiently transfected with the indicated GFP-tagged small GTPase, then infected with either WT or Δ*dotA* *L.p.* for 1 to 4 hours, or left uninfected. Blots were probed with anti-GFP and anti-Hsp70 antibodies. Monoubiquitinated GTPase indicated with an arrow.

Figure 3-S1: Sequence alignment of ubiquitinated small GTPases with UB sites indicated. Related to Figure 3. Sequence alignment of small GTPases ubiquitinated during infection. 61 of 63 ubiquitinated small GTPases represented, with RRAGC and ARL13B omitted for visual clarity

due to their significant length. Sequence colored by conservation within the small GTPase superfamily, from white (non-conserved) to black (extremely highly conserved residue). Ubiquitinated residues at either 1- or 8-hours post infection are colored in bright pink and outlined in black, and deubiquitinated residues are colored in dark blue. Structural and functional regions indicated above, using Rab1A as an example. Regions frequently ubiquitinated across detected small GTPases are underlined in pink and numbered 1-10. ARL13B_K39 and RRAGC_K79 fall in UB region #2. ARL13B_K203 falls in UB region #10.

Figure 4-S1: Rab10 ubiquitination is not controlled by DrrA and requires membrane association. (A) Immunoblot analysis of lysates prepared from HEK293T FcγR transfected with 3XFlag Rab10 and infected with a Δ*drrA L.p*. strain panel (WT, Δ*dotA*, Δ*drrA*, and Δ*drrA* complemented with empty vector or plasmid encoded DrrA WT or D110, 112A) for 1 hour (MOI=50). Monoubiquitinated Rab10 indicated with an arrow. **(B)** Quantification of biological replicates (N=3) of experiment shown in (A). Normalized Rab10 monoubiquitination intensity was calculated as a percentage of WT *L.p.* infection levels (see Methods). **(C)** Immunoblot analysis of monoubiquitination of Rab10 WT vs ΔCAAX during *L.p.* infection. HEK293T FcγR cells were transfected with either 3X Flag Rab10 WT or ΔCAAX, then infected with WT or Δ*dotA L.p.* for 1 hour (MOI=50) or left uninfected. Lysates were probed with anti-Flag antibody. Monoubiquitinated Rab10 indicated with an arrow.

Figure 5-S1: Rab5 ubiquitination reproduces across cell lines and isoforms and is dependent upon membrane localization. Related to Figure 5. (A) Immunoblot analysis of lysates prepared from HEK293T FcγR transfected with 3XFlag Rab5A and infected with *L.p.* WT or Δ*dotA*. **(B)** Immunoblot analysis of lysates prepared from HeLa FcγR transfected with 3XFlag Rab5A and infected with *L.p.* WT or Δ*dotA*. **(A)** Immunoblot analysis of lysates prepared from HEK293T FcγR transfected with 3XFlag Rab5B or 3XFlag Rab5C and infected with *L.p.* WT or Δ*dotA.* **D)** and **(E)** Immunofluorescence analysis of mCherry Rab5A WT or ΔCAAX LCV recruitment. HeLa FcγR cells were transfected with indicated construct, then infected for 1 hour with either WT or Δ*dotA L.p.*, fixed, and stained with anti-*Legionella* antibody. **(D)** Representative images, and **(E)** quantification of mCherry positive LCVs as in (D). **(F)** Immunoblot analysis of ubiquitination of Rab5A WT vs ΔCAAX during *L.p.* infection. HEK293T FcγR cells were transfected with either 3X Flag Rab5A WT or ΔCAAX, then infected with WT or Δ*dotA L.p.* for 4 hours or left uninfected. Lysates were probed with anti-Flag antibody. **(G)** Quantification of normalized Rab5A ΔCAAX mUb intensity as a percent of Rab5A WT mUb during WT *L.p.* infection (see Methods). Biological replicates (N=4) were carried out as in (G). *For all bar graphs:* bars represent mean value, error bars represent standard deviation. Individual points are values from each biological replicate. *Statistical analysis of LCV scoring quantification:* G test of independence was performed on pooled counts (positive vs. negative) from all biological replicates. Upon verifying significance ($p<0.05$), pairwise comparisons between strains were evaluated by post-hoc G-test using the Bonferroni-adjusted p-value as a significance threshold ($p = 0.008$). * = $p<0.008$, ** = $p<0.0008$, *** = $p<0.00008$, n.s. = $p>0.008$.

Figure 7-S1: Rab1 ubiquitination is primarily promoted by SdcA. Related to Figure 7. (A) Immunoblot analysis of lysates prepared from HEK293T FcγR transfected with 3XFlag Rab1A and infected with a Δ*sidC/sdcA L.p*. strain panel (WT, Δ*dotA*, Δ*sidC/sdcA*, and Δ*sidC/sdcA* complemented with empty vector or plasmid encoded SdcA or SidC) for 1 hour (MOI=50). **(B)** Quantification of biological replicates (N=3) of experiment shown in (A). Normalized Rab1A monoubiquitination intensity was calculated as a percentage of WT *L.p.* infection levels (see Methods).

Figure 7-S2: Small GTPases with detected ubiquitinations overlap with mammalian small GTPases known to be recruited to the LCV. Related to Figure 7. Compiled list of (1) small GTPases with detected ubiquitination in our ubiquitinomics data and (2) mammalian small GTPases known to be recruited to the LCV as assessed by immunofluorescent and/or purified LCV mass spectrometry approaches. Data type indicators: (+) detected via mass spectrometry of purified LCV, (•) detected via immunofluorescence, (ø) not detected via immunofluorescence. Sources: **(1)** (Clemens *et al.*, 2000a) **(2)** (Kagan and Roy, 2002) **(3)** (Nagai *et al.*, 2002) **(4)** (Derré and Isberg, 2004) **(5)** (Kagan *et al.*, 2004) **(6)** (Hoffmann *et al.*, 2014) **(7)** (Bruckert and Kwaik, 2015) **(8)** (Schmölders *et al.*, 2017) **(9)** (Jeng *et al.*, 2019) **(10)** (Liu *et al.*, 2020) **(11)** (Kawabata *et al.*, 2021).

Figure 7-S3: Small GTPases with detected ubiquitinations overlap with *Dictyostelium* small GTPases known to be recruited to the LCV. Related to Figure 7. Compiled list of *Dictyostelium* (amoebal) small GTPases known to be recruited to the LCV as assessed by immunofluorescent and/or purified LCV mass spectrometry approaches. Data type indicators: (+) detected via mass spectrometry of purified LCV, (•) detected via immunofluorescence, (ø) not detected via immunofluorescence. Closest human homologues were determined via Dictybase (http://dictybase.org/) and/or protein BLAST. Sources: **(1)** (Urwyler *et al.*, 2009) **(2)** (Rothmeier *et al.*, 2013) **(3)** (Hoffmann *et al.*, 2014) **(4)** (Schmölders *et al.*, 2017) **(5)** (Vormittag *et al.*, 2023).

Supplemental Table 1 – HPLC and MS methods.xlsx

Supplemental Table 2 – Infection Proteomics Dataset.xlsx

Supplemental Table 3 – Pathway and Protein Complex Enrichment Analysis.xlsx

A)

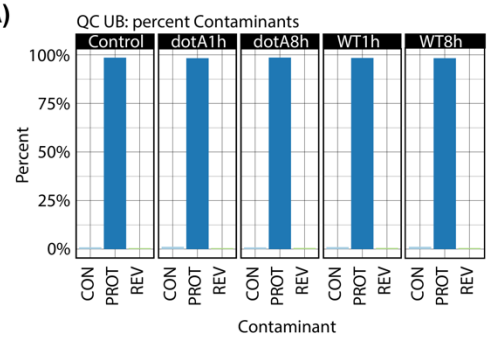

B)

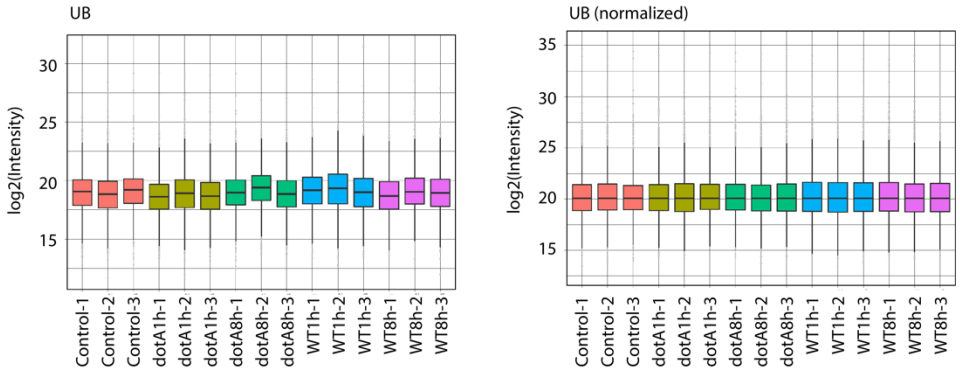

C)

Dataset	Sample	# bioreplica	# bioreplica	n (# peptides)	r (correlation coefficient)
UB	Control	1	2	3000	0.8
UB	Control	1	3	3000	0.85
UB	Control	2	3	3000	0.88
UB	WT1h	1	2	4034	0.91
UB	WT1h	1	3	4034	0.88
UB	WT1h	2	3	4034	0.88
UB	WT8h	1	2	3527	0.9
UB	WT8h	1	3	3527	0.89
UB	WT8h	2	3	3527	0.91
UB	dotA1h	1	2	2728	0.89
UB	dotA1h	1	3	2728	0.87
UB	dotA1h	2	3	2728	0.86
UB	dotA8h	1	2	3241	0.87
UB	dotA8h	1	3	3241	0.9
UB	dotA8h	2	3	3241	0.88

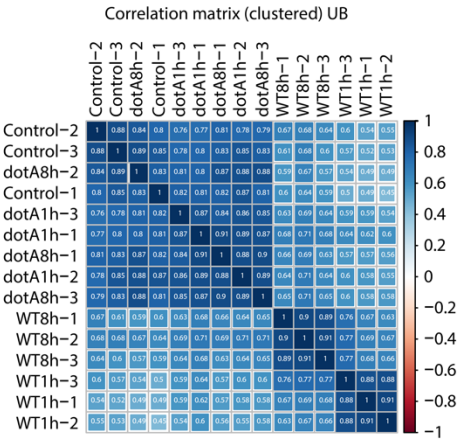

D)

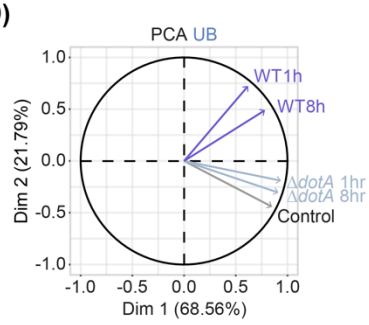

Figure 1S1: Quantification and quality control plots of ubiquitinomics data. Related to Figure 1.

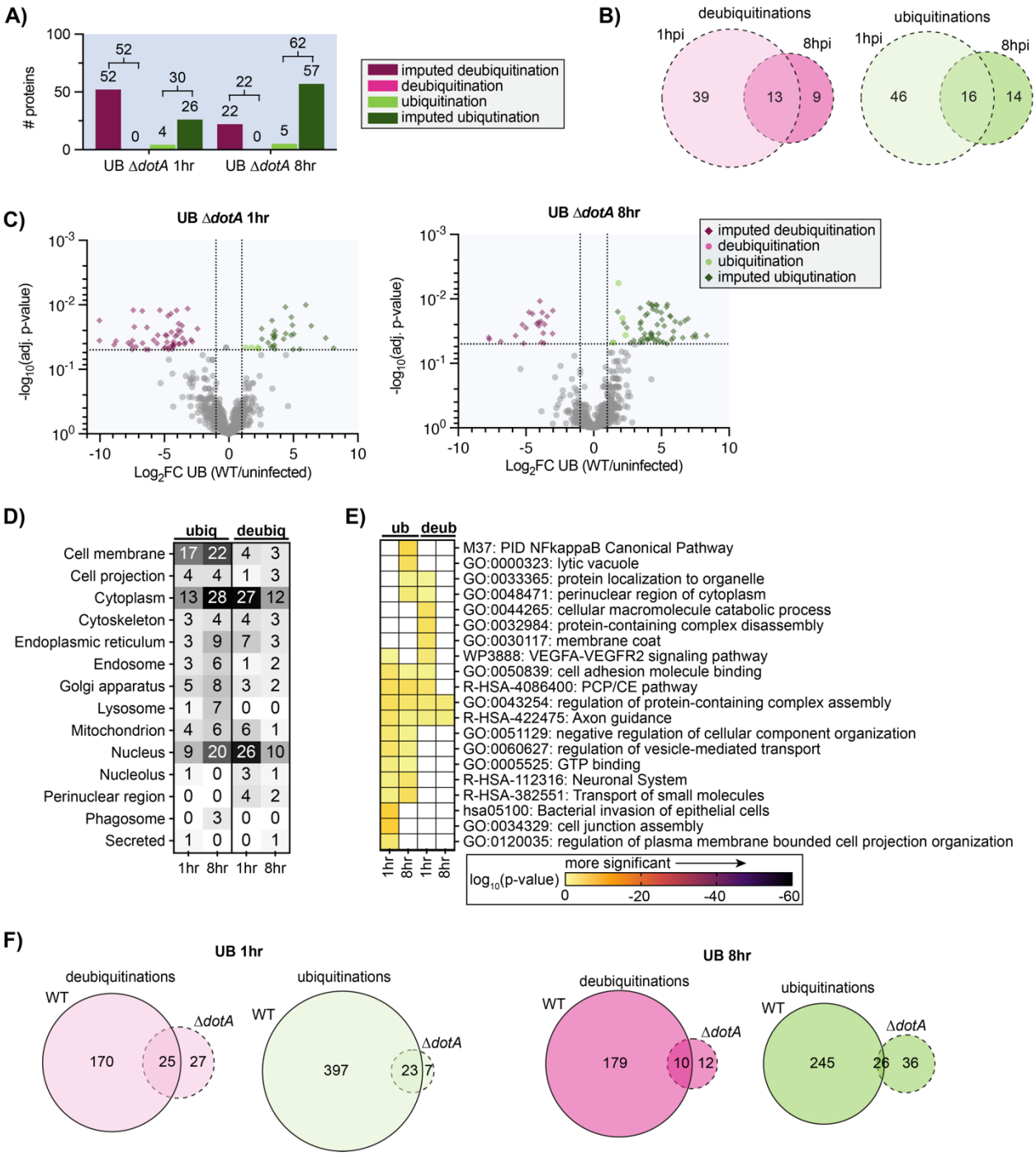

Figure 1S2: Analysis of T4SS-independent (*L.p.* Δ*dotA*) changes in the host cell ubiquitinome. Related to Figure 1

A)

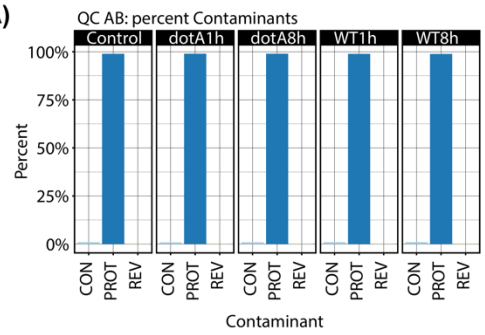

B)

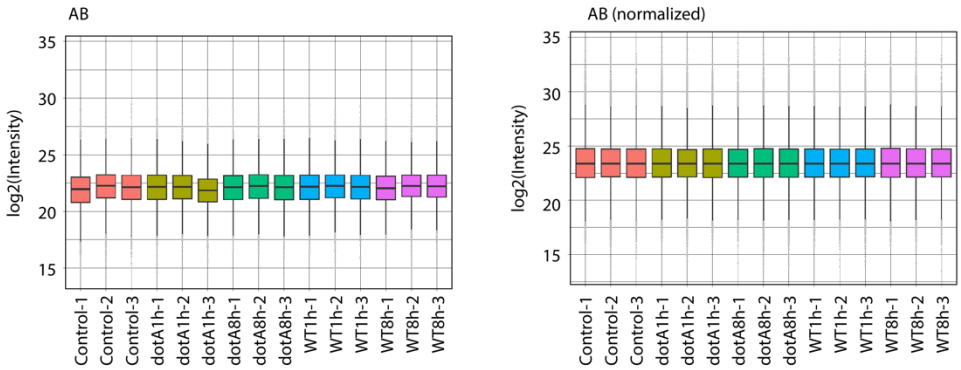

C)

Dataset	Sample	# bioreplica	# bioreplica	n (# peptides)	r (correlation coefficient
AB	Control	1	2	35755	0.86
AB	Control	1	3	35755	0.88
AB	Control	2	3	35755	0.9
AB	WT1h	1	2	40087	0.87
AB	WT1h	1	3	40087	0.86
AB	WT1h	2	3	40087	0.87
AB	WT8h	1	2	40748	0.84
AB	WT8h	1	3	40748	0.84
AB	WT8h	2	3	40748	0.89
AB	dotA1h	1	2	39605	0.85
AB	dotA1h	1	3	39605	0.79
AB	dotA1h	2	3	39605	0.8
AB	dotA8h	1	2	40096	0.86
AB	dotA8h	1	3	40096	0.86
AB	dotA8h	2	3	40096	0.88

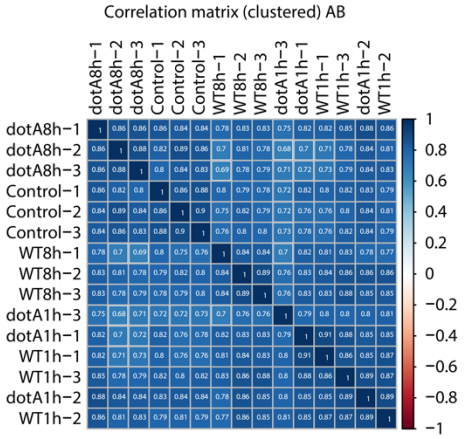

D)

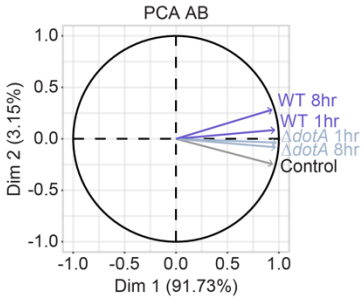

Figure 1S3: Quantification and quality control plots of abundance data. Related to Figure

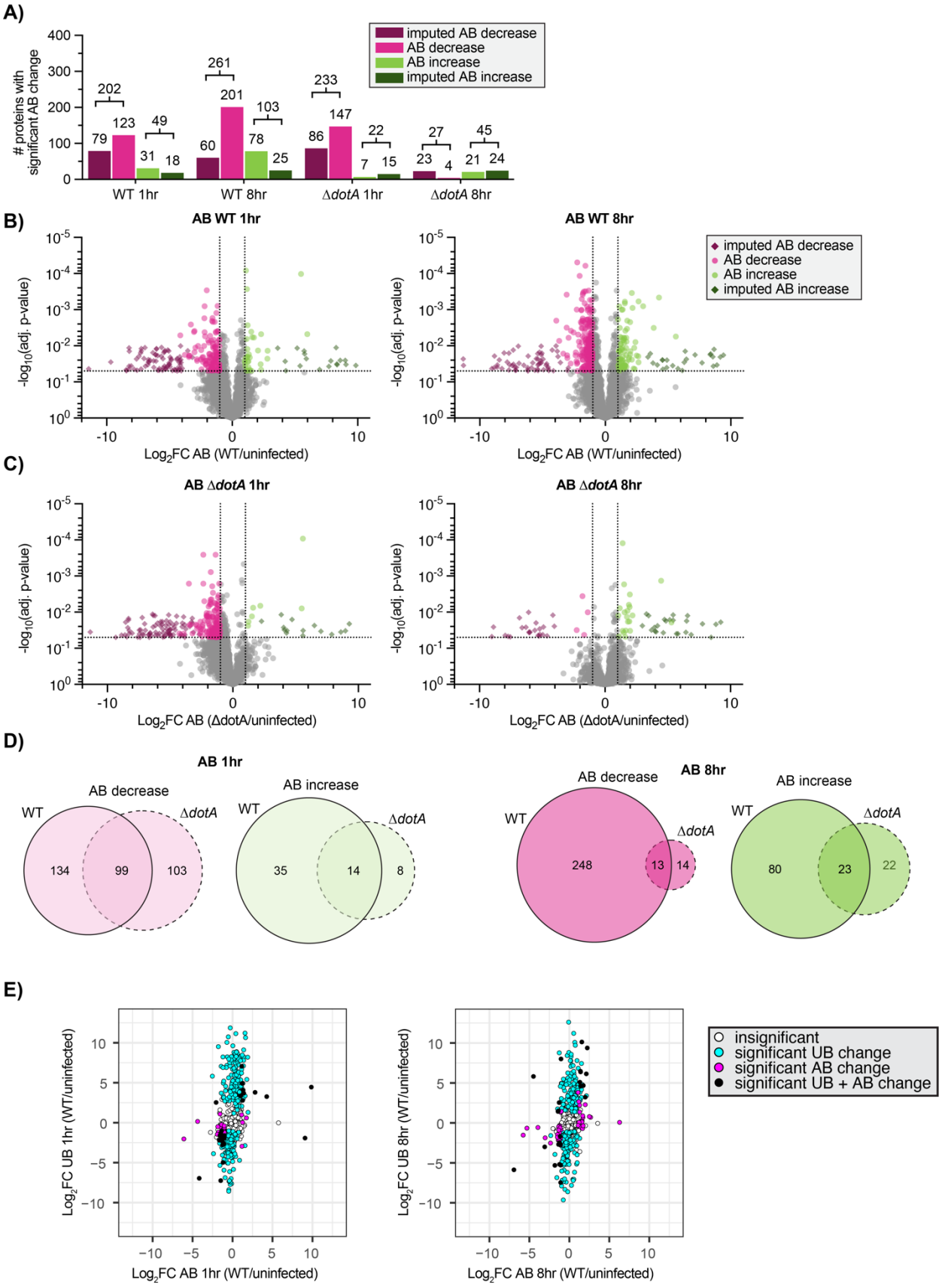

Figure 1S4: Analysis of *L.p.*-induced changes in host cell abundance. Related to Figure 1.

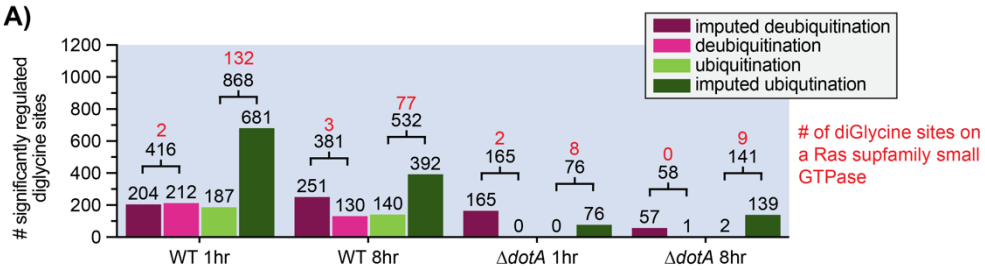

Figure 2S1: Quantification of diglycine site data. Related to Figure 2.

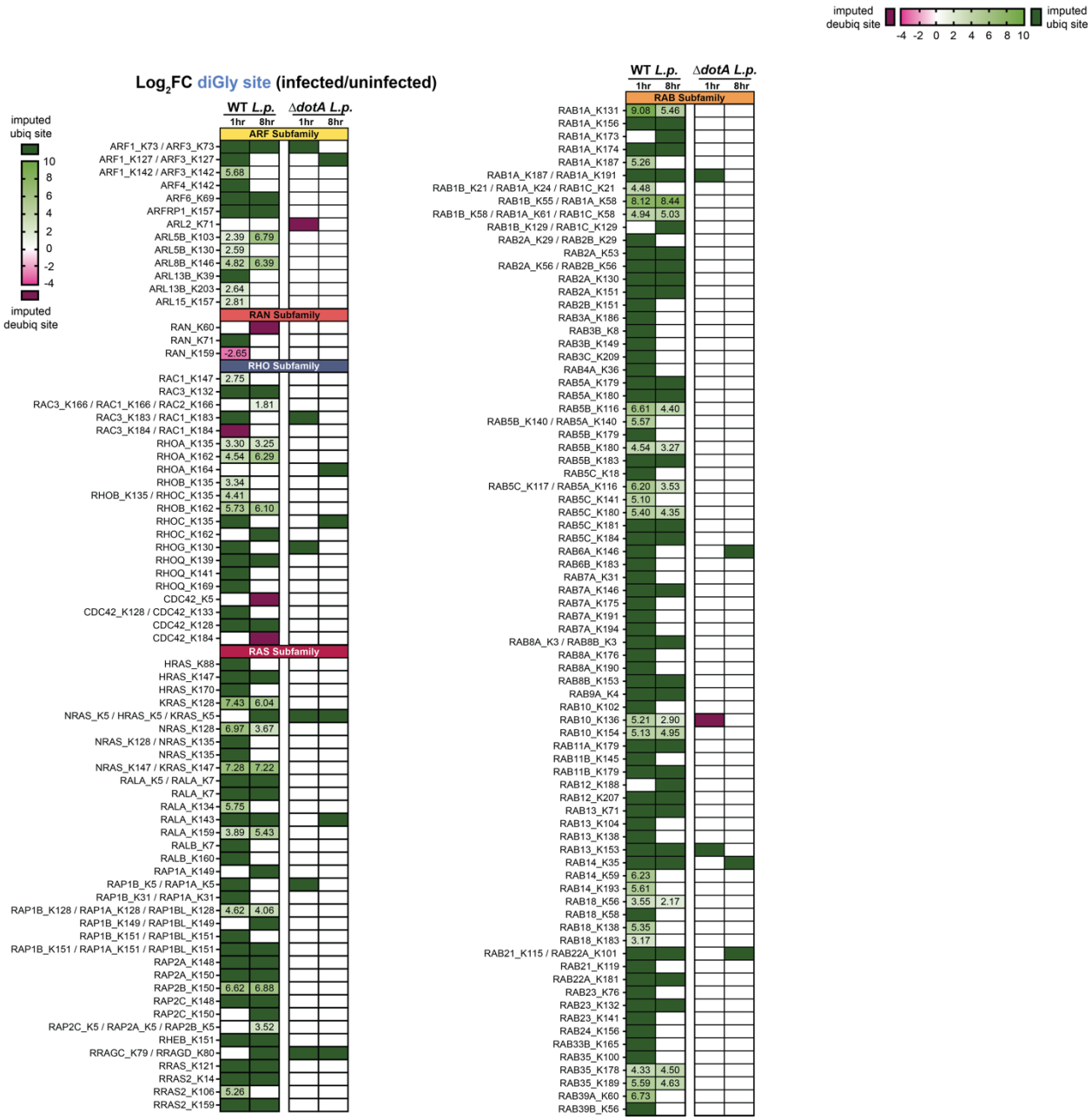

Figure 2S2: List of significantly regulated diGly sites falling on small GTPases. Related to Figure 2.

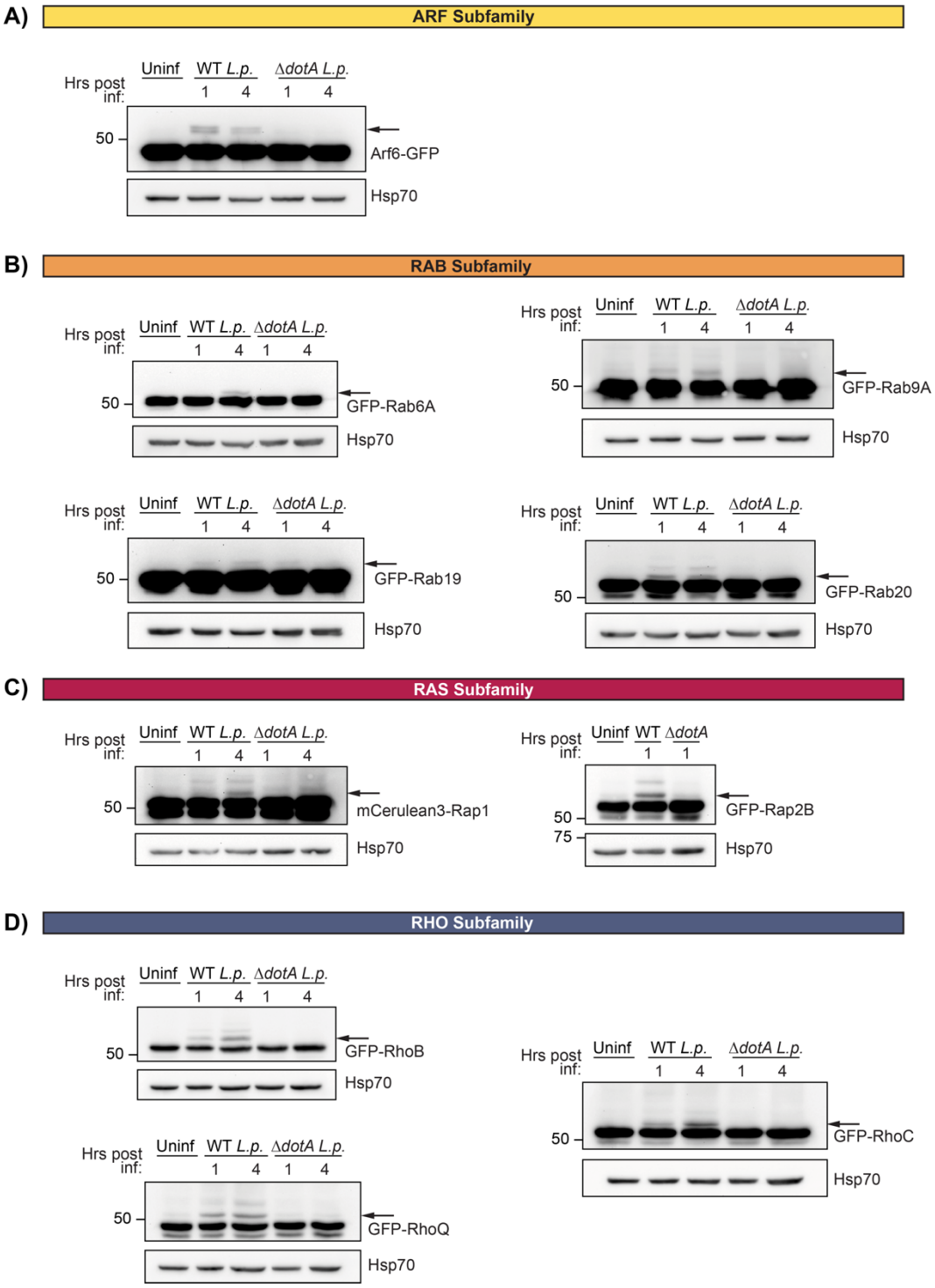

Figure 2S3: Extended immunoblot analysis of small GTPase ubiquitination confirmations. Related to Figure 2.

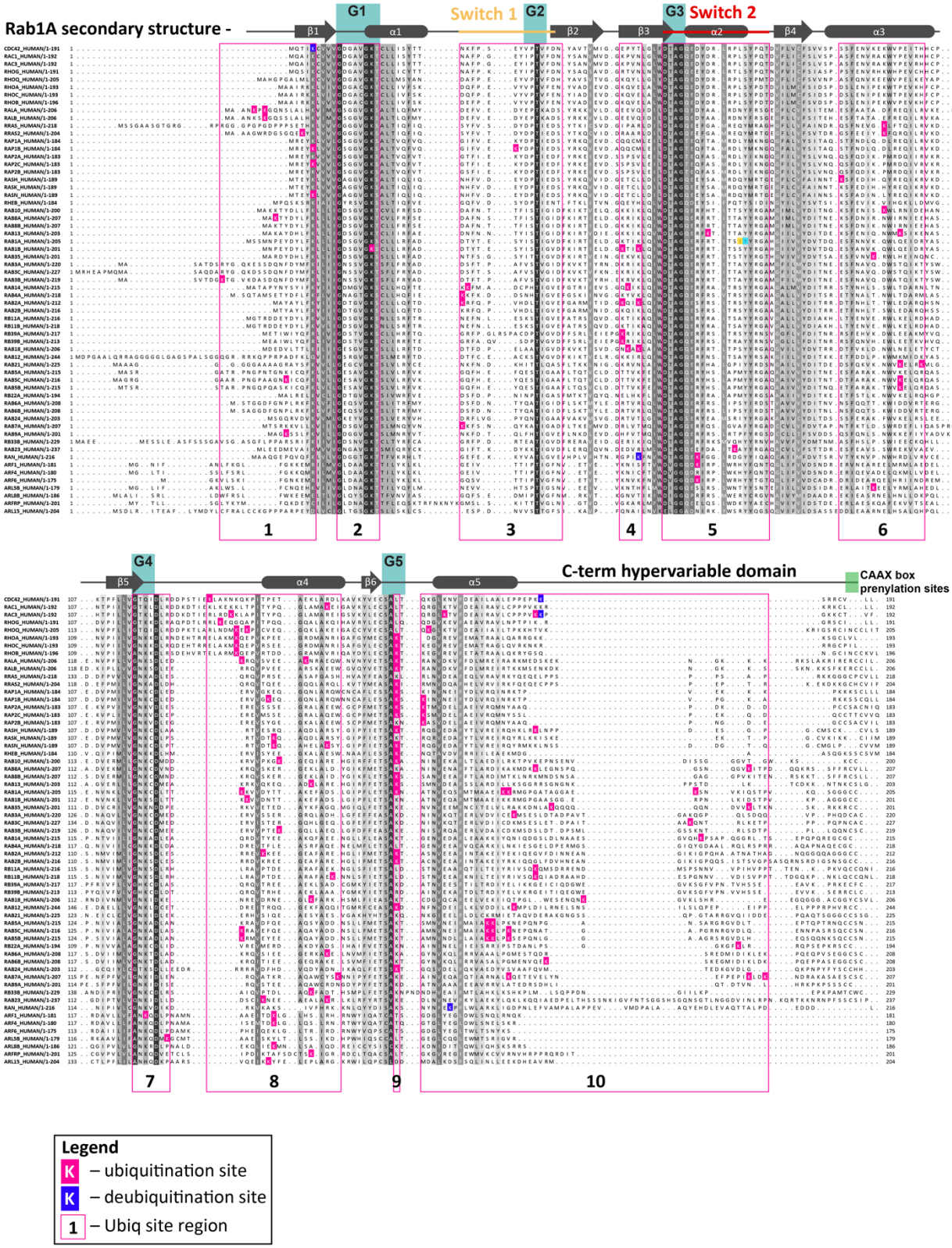

Figure 3S1: Sequence alignment of ubiquitinated small GTPases with UB sites indicated. Related to Figure 3.

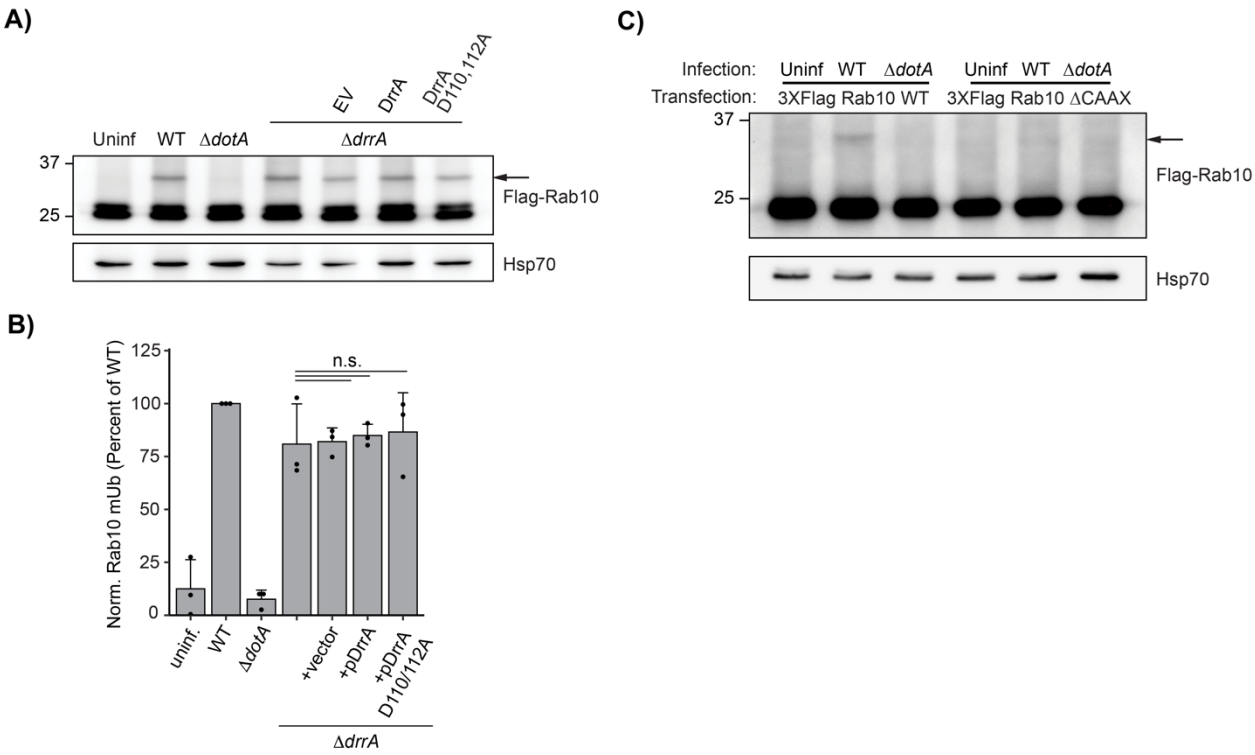

Figure 4S1: Rab10 ubiquitination is not controlled by DrrA and requires membrane association. Related to Figure 4.

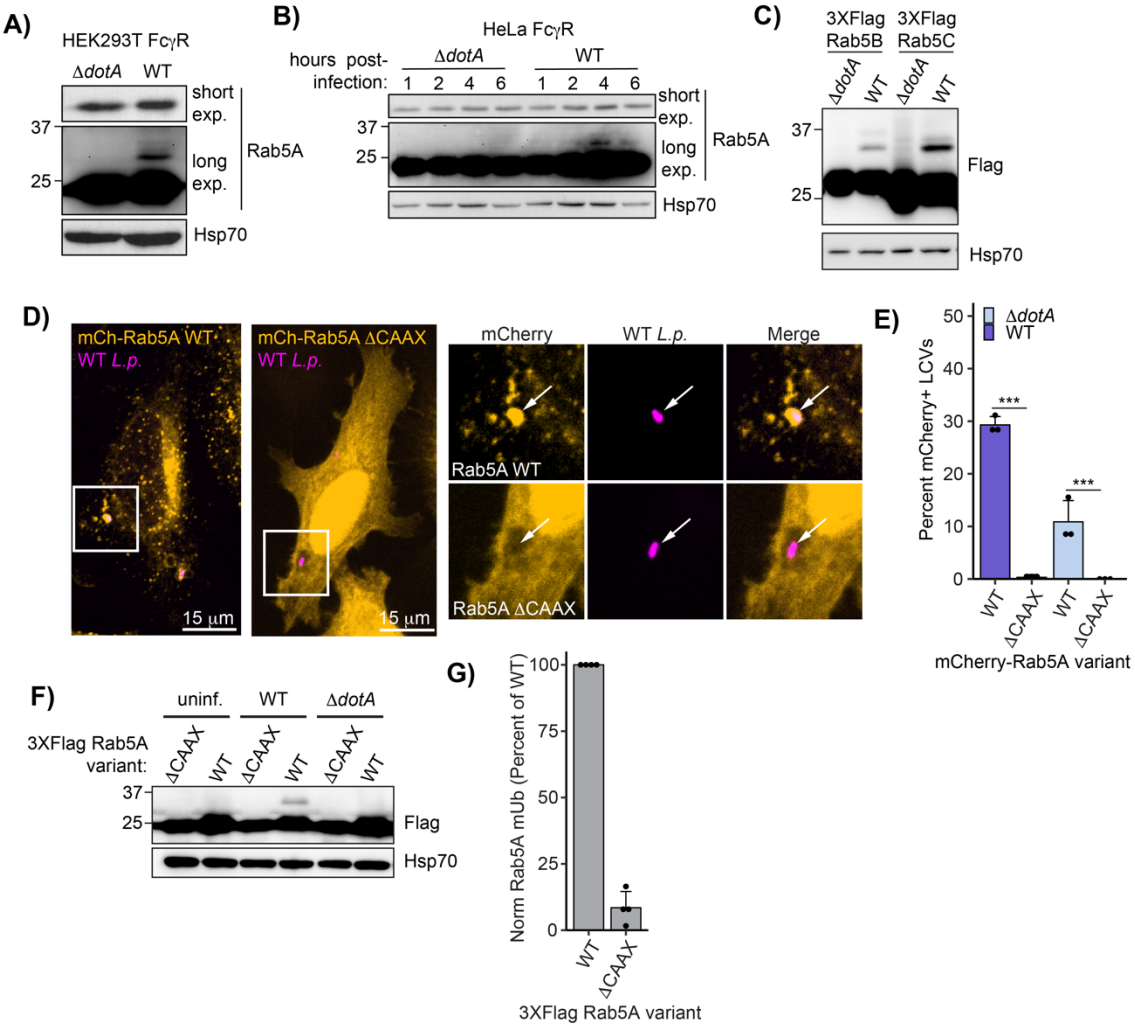

Figure 5S1: Rab5 ubiquitination reproduces across cell lines and isoforms and is dependent upon membrane localization. Related to Figure 5.

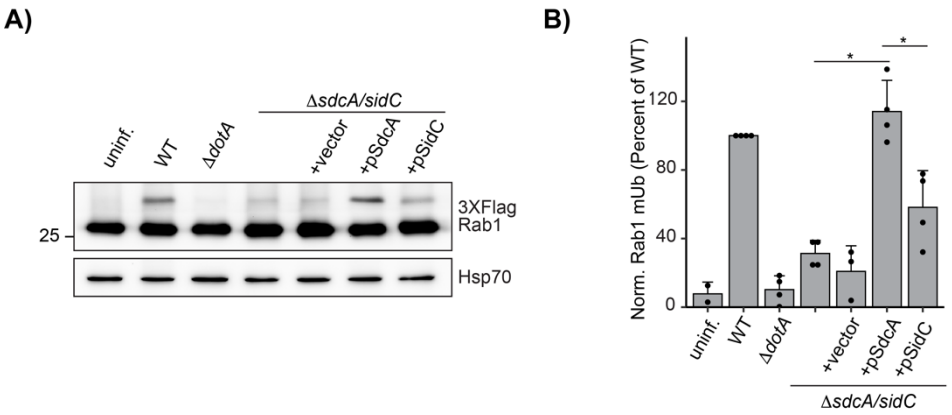

Figure 7S1: Rab1 ubiquitination is primarily promoted by SdcA. Related to Figure 7.

Mammalian GTPase LCV recruitment data

Legend

+	Detected in purified LCV proteomics
•	Detected on LCV via immunofluorescence
ø	Not detected on LCV via immunofluorescence

Small GTPase	Ubiq during WT *L.p.* infection	Documented recruitment to WT LCV	LCV Recruitment Source and Data Type														
			source	1	2	3	4	5	6		7	8		9	10	11	this study
			data type	IF	IF	IF	IF	IF	MS	IF	MS	MS	IF	IF	IF	IF	IF
			host cell	HeLa	BMDM / CHO Fcg	BMDM	BMDM / COS Fcg	BMDM / CHO Fcg	RAW264.7	RAW264.7	U937	RAW264.7	RAW264.7	HeLa Fcg	MLE	HeLa Fcg	HeLa Fcg
ARF1	x	x			•	•	•		+		+						
ARF3		x										+					
ARF4	x	x									+						
ARF6	x	x									+						
ARFRP1	x																
ARL5B	x																
ARL8A		x										+					
ARL8B	x	x							+								
ARL13B	x																
ARL15	x																
RAB1A	x	x					•	•	+		+	+					
RAB1B	x	x							+			+					
RAB2A	x	x					ø	ø	+	•	+	+					
RAB2B	x																
RAB3A	x																
RAB3B	x																
RAB3C	x																
RAB4A	x	x								•							
RAB4B		x							+								
RAB5A	x	x							+	•		+					•
RAB5B	x	x									+	+					
RAB5C	x	x		ø					+		+	+					
RAB6A	x	x						ø	+	ø		+				•	
RAB6B	x																
RAB7A	x	x							+	•	+	+					
RAB8A	x	x							+								
RAB8B	x	x							+			+					
RAB9A	x	x								•							
RAB10	x	x							+	•	+	+		•	•		
RAB11A	x	x							+	•	+	+					
RAB11B	x																
RAB12	x																
RAB13	x																
RAB14	x	x							+		+	+					
RAB18	x	x							+	ø		+					
RAB21	x	x							+	•		+					
RAB22A	x																
RAB23	x																
RAB24	x																
RAB27A																	
RAB31		x							+			+					
RAB32		x								•							
RAB33B	x	x														•	
RAB35	x																
RAB39A	x																
RAB39B	x																
RABL6		x									+						
RAN	x	x									+						
HRAS	x																
KRAS	x	x							+								
NRAS	x																
RAP1A	x	x									+	+	•				
RAP1B	x	x									+						
RAP2A	x	x									+						
RAP2B	x																
RAP2C	x	x										+					
RHEB	x																
RRAS	x																
RRAS2	x																
RALA	x	x									+						
RALB	x	x									+						
RRAGC	x																
RAC1	x	x									+						
RAC2		x							+		+						
RAC3	x																
RHOA	x	x									+						
RHOB	x																
RHOC	x																
RHOG	x	x									+	+					
RHOQ	x																
CDC42	x	x									+						
RHOT1		x							+								

Figure 7S2: Small GTPases with detected ubiquitinations overlap with mammalian small GTPases known to be recruited to the LCV. Related to Figure 7.

Dictyostellium GTPase LCV recruitment data

Legend

+	Detected in purified LCV proteomics
•	Detected on LCV via immunofluorescence
ø	Not detected on LCV via immunofluorescence

Documented recruitment to WT LCV in *Dictyostellium*	Closest Human Homologue (Dictybase/BLAST)	Mammalian Homologue Ubiq during WT *L.p.* infection	LCV Recruitment Source and Data Type							
			source	1		2	3		4	5
			data type	MS	IF	IF	MS	IF	MS	MS
ARFA	ARF1	x		+			+			
ARL8	ARL8A, ARL8B	x								+
SARA	SAR1A						+			+
RAB1A	RAB1A, RAB1B	x		+	•		+			
RABG2	RAB1A	x								+
RAB1B	RAB1B	x								+
RABC	RAB1A, RAB1B	x		+						+
RAB1D	RAB1A, RAB1B	x		+			+			+
RAB2A	RAB2A	x					+		+	+
RAB2B	RAB2B	x					+		+	+
RABQ	RAB2B, RAB2A	x								+
RAB4	RAB4A	x								+
RAB5A	RAB5A	x					+	•	+	+
RAB5B	RAB5B	x						•	+	+
RAB6	RAB6A	x					+		+	+
RAB7A	RAB7A	x		+	•		+		+	+
RAB8A	RAB8A	x		+	•		+		+	
RAB11A	RAB11A	x					+		+	+
RAB11B	RAB11B	x						•		
RAB11C	RAB11B	x						•	+	+
RAB14	RAB14	x		+	•		+		+	
RAB18	RAB18	x					+			+
RAB32A	RAB32, RAB38	x					+		+	+
RAB32B	RAB32	x								+
RAB32C	RAB32	x								+
RAB32D	RAB32	x								+
RANA	RAN	x		+		•	+		+	+
RASB	KRAS	x								+
RASC	KRAS	x								+
RASG	KRAS	x		+			+		+	+
RASS	KRAS	x								
RAPA	RAP1A, RAP1B	x					+		+	+
RAC1A	RAC1	x								+
RACB	RAC1	x					+			+
RACC	RAC1	x								+
RACE	RAC1	x					+			+
GEMA	RHOT1								+	+

Figure 7S3: Small GTPases with detected ubiquitinations overlap with *Dictyostelium* small GTPases known to be recruited to the LCV. Related to Figure 7.